

Particle Collection Efficiency in a Venturi Scrubber: Comparison of Experiments with Theory

Stephen N. Rudnick,* John L. M. Koehler, Kenneth P. Martin, David Leith,[†] and Douglas W. Cooper[‡]

Physical Sciences and Engineering Program, Harvard University School of Public Health, Boston, Massachusetts 02115

■ Particle collection efficiencies in 23 size intervals covering a diameter range of 0.32–2.8 μm were measured for venturi scrubbers with throat diameters of 3.2, 5.4, and 7.6 cm. Each scrubber was operated with four types of liquid injection, throat gas velocities from 21 to 160 m/s, and liquid-to-gas volume ratios from 0.00019 to 0.0043. Results were compared to three widely used theoretical models using a least-squares performance index. Yung's model predicted the data better than either Calvert's model with $f = 0.25$, the recommended value for collection of hydrophobic particles in laboratory-scale venturi scrubbers, or Boll's model. In addition, the performance of each model improved with increasing throat diameter. Complete performance data, including pressure drop, are reported in supplementary material and should prove useful for improving and validating venturi scrubber models.

Introduction

Venturi scrubbers are used widely for removing particles from gases because of their many attractive features: they remove submicrometer particles efficiently; they are compact and simple to build, so that initial investment costs are small in comparison to other types of particle collection devices; and they function well in problematic situations such as hot or corrosive atmospheres and when sticky particles must be collected.

The literature contains a number of models to predict venturi scrubber efficiency; these models are useful in optimizing and designing new venturi scrubbers as well as predicting the effects of changing parameters in existing ones. Some models are explicit, analytical expressions that have straightforward solutions. Others are more complex and require numerical solution with a computer. Few data have been available to confirm model predictions, so model evaluation has been difficult.

The purposes of the present work were to develop data on the performance of venturi scrubbers over a wide range of operating conditions and to compare these data with predictions of venturi scrubber efficiency from several important models. The data should also provide a reference against which future efficiency models can be compared. Evaluation of efficiency models should help determine which one gives the best results and whether the

additional complexity of some models is worthwhile.

Experimental Methods

Three venturis were used; each had a circular cross section with 127-mm-inlet and -outlet diameters and was machined from transparent acrylic plastic. The small-throat venturi had a 251-mm-long converging section, a throat with diameter and length of 32 mm, and a 556-mm-long diverging section; the medium-throat venturi had a 203-mm-long converging section, a 54 mm diameter, 51-mm-long throat, and a 435-mm-long diverging section; the large-throat venturi had a 138-mm-long converging section, a throat with diameter and length of 76 mm, and a 305-mm-long diverging section. These venturis were oriented so that airflow was downward.

A schematic diagram of the experimental system is shown in Figure 1. Airflow rate was controlled with dampers and determined from the pressure drop across a Stairmand disk, which was calibrated over the experimental airflow range by pitot traverses. Incoming air was filtered with a nuclear-grade HEPA filter (1) to remove essentially all particles. The test aerosol, introduced immediately downstream of the HEPA filter, was generated from Wesson oil, a commercial cooking oil with density of 0.92 g/cm³, using a Wright pneumatic nebulizer (2) maintained at an inlet pressure of 30 kPa.

Distilled water was used as the scrubbing liquid. The water was filtered through a Millipore 0.2- μm membrane filter and a MSA 1106BH fiberglass filter in series to minimize the size of particles left from water droplets that evaporated, because such residual particles would confound measurement of Wesson oil particles penetrating the venturi scrubber. Water flow rate was measured with a rotameter and controlled with a valve. Water was injected into the venturi in four ways: (1) circumferentially inward injection: water was introduced 20.9 mm above the entrance of the converging section through an 0.6-mm-wide circumferential slot in the duct wall; (2) circumferentially downward injection: water was introduced downward onto the wall, 15.0 mm above the entrance of the converging section, through a 1.0-mm-wide annular opening; (3) single-nozzle downward injection: water was introduced downward at the converging-section entrance through a concentric 14.2-mm-diameter opening; and (4) multiple-nozzle downward injection: water was introduced downward at the converging-section entrance through 12 4.8-mm-diameter openings arranged to approximate radially uniform water distribution.

* Present address: Department of Environmental Science and Engineering, University of North Carolina, Chapel Hill, NC 27514.

[†] Present address: Manufacturing Research Laboratory, Thomas J. Watson Research Center, IBM, Yorktown Heights, NY 10598.

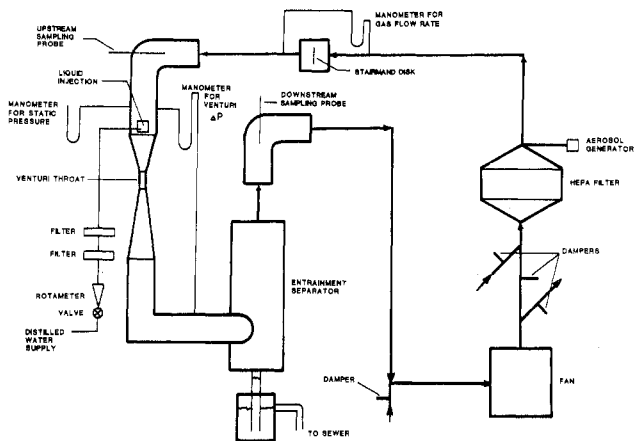


Figure 1. Schematic diagram of venturi scrubber system.

A 305-mm-diameter, 1.22-m-high transparent acrylic-plastic cyclone was used as an entrainment separator. It had a tangential entry whose centerline was 191 mm above the bottom of the cyclone. Water was discharged parallel to the cyclone axis from a 64-mm-diameter opening at the bottom of the cyclone. Air exited from the top of the cyclone, parallel to its axis, through a 127-mm-diameter duct that contained vane straighteners.

Pressure drop across the venturi scrubber was measured with a manometer. One pressure tap was 264 mm upstream of the converging-section entrance, and the other was 387 mm downstream of the inner corner of the mitered 90° elbow that was 1.7 m downstream of the converging-section entrance. The downstream pressure tap, located on top of a 127-mm-diameter horizontal duct, was cleared with compressed air immediately before recording pressure drop, because this tap tended to fill with water and cause erroneous pressure-drop readings.

Isokinetic samples of aerosol were taken through probes of 7.5 mm i.d., as shown in Figure 1. To obtain representative samples, the probes were aligned with the axis of the duct and probe entrances were located at least 7 duct diameters from upstream interferences. Five 2-min samples were taken sequentially for each experimental run. The first and fifth were upstream samples, the second and fourth were downstream samples, and the third was a downstream blank, a sample taken while the aerosol generator output was diverted from the system. This blank gave the contribution to the downstream sample from small water droplets and from impurities in the water remaining from evaporated droplets. Aerosol particles were counted and sized into 23 size intervals covering a diameter range of 0.32–2.8 μm with a classical forward-scattering, optical aerosol spectrometer (3) manufactured by Particle Measuring Systems, Boulder, CO. Penetrations (P_t) for each particle size range were calculated from the following equation:

$$P_t = \frac{c_d - c_b}{c_u} \quad (1)$$

where, for each particle size interval, c_u is upstream number concentration, c_d is downstream number concentration, and c_b is number concentration in the downstream blank. The coefficient of variation in percent (C_v), based on propagation of the error associated with the number of particles counted, was calculated from eq 2, derived elsewhere (4).

$$C_v = 100 \sqrt{\frac{1}{c_u} + \frac{1 + 4c_b/c_d}{c_d(1 - 2c_b/c_d)^2}} \quad (2)$$

Theoretical Models

Many models and correlations have been proposed to predict particle collection efficiency in a venturi scrubber (5–15). We chose the models of Calvert et al. (8), Yung et al. (9), and Boll (10), herein referred to as the Calvert, Yung, and Boll models, to compare with our experimental measurements because these models are the ones most widely quoted. The Calvert and Yung models, which are explicit algebraic formulas, are popular because the necessary calculations are easy to do. The Boll model, which requires computer-aided numerical solution, uses fewer assumptions than the other two models; most sophisticated models are variants of the Boll model.

Liquid Atomization. Calvert et al. (8), Yung et al. (9), and Boll (10) assumed that after injection all liquid atomizes instantaneously into monodisperse droplets with a diameter equal to the Sauter mean diameter, D_d in m, given by the Nukiyama-Tanasawa equation (16):

$$D_d = \frac{0.0050}{|V_{Gt} - V_{di}|} + 0.918 \left(\frac{Q_L}{Q_G} \right)^{3/2} \quad (3)$$

where V_{Gt} is superficial gas velocity in the throat in m/s, V_{di} is liquid velocity parallel to the venturi scrubber axis at the exit of the injectors in m/s, and Q_L and Q_G are volumetric liquid and gas flow rates, respectively.

Calvert Model. To obtain an explicit equation for predicting particle collection efficiency in a venturi scrubber, Calvert et al. (8) assumed that a venturi scrubber consists entirely of a throat in which droplets accelerate to gas velocity (i.e., throat is infinitely long) and that drag coefficient (C_D) can be approximated from Eq 4 where Re

$$C_D = 55/Re \quad (4)$$

is droplet Reynolds number

$$Re = \frac{D_d \rho_G |V_G - V_d|}{\mu_G} \quad (5)$$

where ρ_G is gas density, μ_G is gas viscosity, V_G is gas velocity, and V_d is droplet velocity. They also assumed that single-droplet collection efficiency (η) can be calculated from an approximation of the data of Walton and Woolcock (17) given by eq 6 where K is the impaction parameter,

$$\eta = \left(\frac{K}{K + 0.35} \right)^2 \quad (6)$$

defined as the ratio of particle stopping distance to droplet diameter

$$K = \frac{C_c \rho_p D_p^2 |V_G - V_d|}{18 \mu_G D_d} \quad (7)$$

Here, D_p is particle diameter, C_c is particle Cunningham slip-correction factor, and ρ_p is particle density. They derived the following equation for penetration:

$$P_t = \exp \left\{ \frac{Q_L \rho_L D_d V_{Gt}}{55 Q_G \mu_G K_i} \left[2.8 \ln \left(\frac{0.35 + K_i f}{0.35} \right) + \frac{0.49}{0.35 + K_i f} - 1.4 - 4K_i f \right] \right\} \quad (8)$$

where f is a correlative parameter that ranges from 0.2 to 0.7 (8), ρ_L is liquid density, and K_i is the impaction parameter when $(V_G - V_d) = V_{Gt}$. Droplet diameter is calculated from eq 3 with $V_{di} = 0$. For f , Calvert (18) recommends a value of 0.25 for the collection of hydrophobic

particles in laboratory-scale scrubbers. This value of f was used in our comparison of models.

Yung Model. Yung et al. (9) modified the Calvert model by using more realistic assumptions. For estimating droplet drag coefficient, they chose a relationship suggested by Hollands and Goel (19):

$$C_D = C_{Di} \sqrt{\frac{V_{Gt}}{|V_G - V_d|}} \quad (9)$$

where C_{Di} , the drag coefficient at the throat inlet, is obtained from the "standard curve" (20). Yung et al. assumed that the ratio (V_{de}^*) of droplet velocity at the exit of the throat to gas velocity in the throat is given by eq 10, where

$$V_{de}^* = 2(1 - X^2 + X\sqrt{X^2 - 1}) \quad (10)$$

$X = 1 + 3L_t C_{Di} \rho_G / 16D_d \rho_L$, and L_t is throat length. Particle collection is assumed to take place only in the throat. They derived eq 11, an algebraic formula for calculation of penetration. Equation 11 is more complex than eq 8, but

$$Pt = \exp \left\{ \frac{Q_L \rho_L}{Q_G \rho_G C_{Di}} \left([4K_i(1 - V_{de}^*)^{1.5} + 2.1(1 - V_{de}^*)^{0.5} - 3.55K_i^{0.5}(1 - V_{de}^* + 0.35/K_i) \tan^{-1} (K_i(1 - V_{de}^*)/0.35)^{0.5}] / [0.35 + K_i(1 - V_{de}^*)] - [2.1 + 4K_i - 3.55K_i^{0.5}(1 + 0.35/K_i) \tan^{-1} (K_i/0.35)^{0.5}] / [0.35 + K_i] \right) \right\} \quad (11)$$

does not require the correlative parameter, f .

Boll Model. Boll (10) assumed that after liquid atomization each droplet accelerates and decelerates in response to the drag force from the gas, according to Newton's second law of motion. He assumed one-dimensional flow parallel to the venturi scrubber axis for gas and droplets and used the "standard curve" in tabular form for C_D (20). He used eq 12-14 to describe droplet motion. In eq 12-14

$$a_d = \frac{3\rho_G C_D}{4\rho_L D_d} (V_G - V_d) |V_G - V_d| \quad (12)$$

$$V_d = V_{di} + \int_0^t a_d dt \quad (13)$$

$$x = x_i + \int_0^t V_d dt \quad (14)$$

a_d is droplet acceleration, t is time, and x is droplet displacement along the venturi scrubber axis from x_i , the point of liquid injection. Because Boll assumed that droplets having a single diameter, given by eq 3, form immediately upon injection, his model has an inherent inconsistency: if the gas velocity in the throat is used to calculate droplet diameter, as was done when the Boll model was tested in this paper, then calculation of penetration through the converging section is based on an incorrect droplet diameter. Boll did not discuss this inconsistency.

As droplets move relative to the gas, they pass through a cylindrical volume equal to the integral product of droplet cross-sectional area, relative velocity between gas and droplet, and time. Boll assumed the fraction of particles collected in this gas volume is given by the theoretical calculations of Dorsch et al. (21), reported by Ranz (22) as a graph of single-droplet collection efficiency vs. impaction parameter. The cumulative effect of all droplets

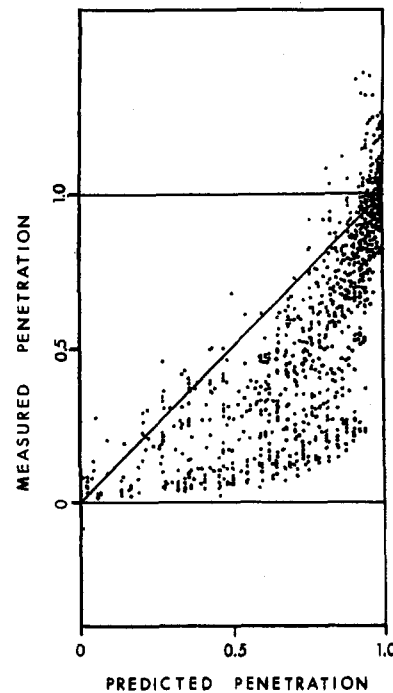


Figure 2. Measured penetration vs. predicted penetration from the Calvert model with $f = 0.25$.

on particle penetration through the venturi scrubber, assuming cross sectional homogeneity, is given by eq 15.

$$Pt = \exp \left(-\frac{3Q_L}{2Q_G D_d} \int_0^t \eta |V_G - V_d| dt \right) \quad (15)$$

Solutions to the above equations depend on venturi scrubber geometry and operating conditions and require numerical methods. Starting with initial values of V_G and V_{di} , one calculates a_d , V_d , and x from eq 12-14 for a small increment of time; gas velocity is then recalculated from the venturi scrubber cross-sectional area and the procedure repeated until the exit of the scrubber is reached. Simultaneously, eq 15 is integrated numerically for each desired particle size to give penetrations.

Results and Discussion

Data. Operating parameters, pressure drops, and measured penetrations with coefficients of variation due to counting errors are listed in the supplementary material for all experimental runs (see paragraph at end of paper regarding supplementary material). A total of 1183 measurements of penetration were made. For some runs, eq 1 gave penetrations less than zero or greater than one. This sometimes occurred because penetration measurements are imprecise when few particles are counted (4). Data from runs where counting errors were large were discarded, based on criteria specified in the supplementary material.

Scatter plots of measured penetration vs. predicted penetration based on the Calvert model with $f = 0.25$, the Yung model, and the Boll model are given in Figures 2-4. These plots suggest that the Yung model performed the best, followed by the Boll and Calvert models, respectively. A more objective analysis follows.

Performance Index. For assessing relative rather than absolute changes in separation operations, penetration is often expressed as a number of transfer units (N),

$$N = -\ln Pt \quad (16)$$

This transformation gives equal weight to the same percentage changes at low and high penetration. After applying this transformation to our data, a least-squares

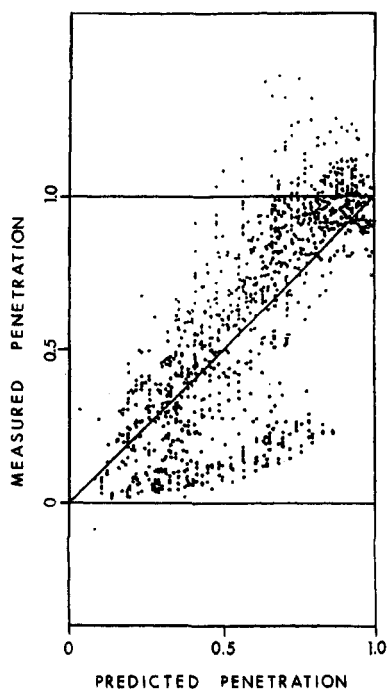


Figure 3. Measured penetration vs. predicted penetration from the Yung model.

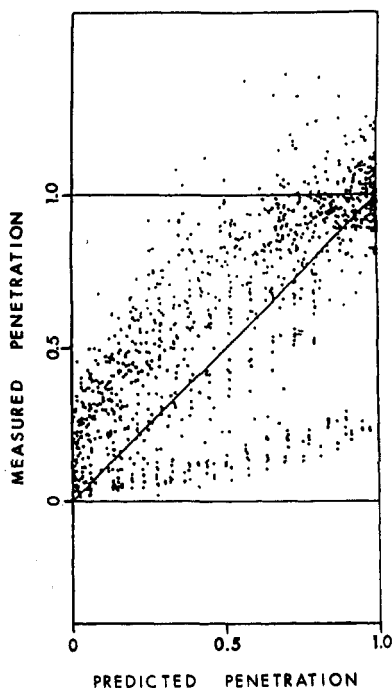


Figure 4. Measured penetration vs. predicted penetration from the Boll model.

performance index, I , was calculated for each theoretical model as follows:

$$I = \frac{\sum_{i=1}^n (N_m - N_p)^2}{n} = \frac{\sum_{i=1}^n \Delta^2}{n} \quad (17)$$

where N_m is the measured number of transfer units, N_p is the predicted number of transfer units, Δ is $(N_m - N_p)$, and n is the number of measured penetrations. The performance index is similar to the quantity minimized when a regression line is fit to data by the method of least squares. Other investigators have employed the performance index for model evaluation (23-25); the objective is to identify a model that minimizes I .

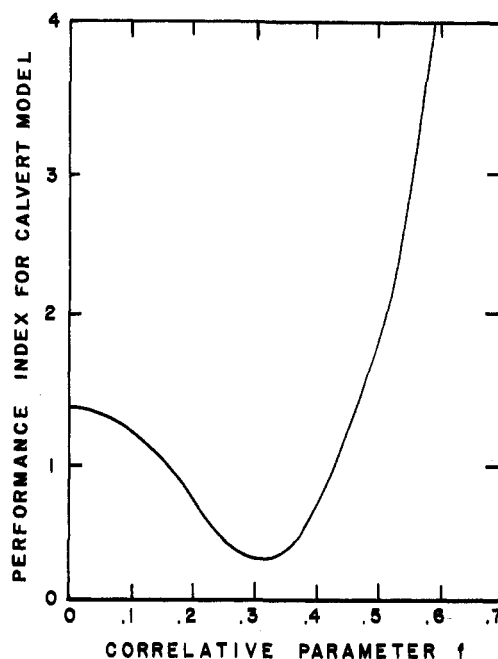


Figure 5. Performance index for the Calvert model vs. Calvert's correlative parameter, f .

Table I. Results of Comparison between Experimental Data and Theoretical Models^a

model	$\bar{\Delta}$	I
Yung	0.143	0.427
Calvert ($f = 0.31$)	0.225	0.433
Calvert ($f = 0.25$)	0.431	0.574
Boll	-0.258	0.880

^aBetter performing models listed first.

The performance index has two components. By definition, σ_{Δ}^2 , the variance of Δ , is

$$\sigma_{\Delta}^2 = \frac{\sum_{i=1}^n (\Delta - \bar{\Delta})^2}{n-1} = \frac{\sum_{i=1}^n \Delta^2}{n-1} - \frac{(\sum_{i=1}^n \Delta)^2}{n(n-1)} \quad (18)$$

where $\bar{\Delta}$ is the mean difference between N_m and N_p over n measurements. If n is large, substitution of eq 17 into 18 yields

$$I = \bar{\Delta}^2 + \sigma_{\Delta}^2 \quad (19)$$

Thus, the two components of I are $\bar{\Delta}$, a measure of the average difference between N_m and N_p (if $\bar{\Delta}$ is positive, model overestimates penetration; if $\bar{\Delta}$ is negative, model underestimates penetration), and σ_{Δ} , a measure of the scatter about the $N_m = N_p$ line (these lines are shown in Figures 2-4). For a model that predicts the data well, both $\bar{\Delta}$ and σ_{Δ} will be small.

Comparison of Models. Four models were included in our comparison: the three models discussed above and the Calvert model with a value of f that minimizes the performance index for our data. As shown in Figure 5, this f value was 0.31. Table I gives values of $\bar{\Delta}$ and I for each model. All models except the Boll model tended to overestimate measured penetrations on average, as shown by the sign of $\bar{\Delta}$. To compare the performance of the four models, two-sided t tests were conducted on I using each of the six possible model pairs.

The performance index for the Boll model was significantly higher (worse) than the index for each of the other models ($p < 0.001$); that is, the Boll model was inferior to the other three models in predicting our data. The performance index for the Calvert model with $f = 0.25$ was

Table II. Effect of Throat Diameter on Comparison of Experimental Data with Theoretical Models

throat diameter	Yung		Calvert ($f = 0.31$)		Calvert ($f = 0.25$)		Boll	
	$\bar{\Delta}$	I	$\bar{\Delta}$	I	$\bar{\Delta}$	I	$\bar{\Delta}$	I
small (32 mm)	1.32	1.93	0.945	1.83	1.44	2.46	0.751	1.52
medium (54 mm)	-0.0346	0.0926	0.167	0.209	0.384	0.280	-0.687	1.20
large (76 mm)	-0.213	0.0854	-0.0460	0.0274	0.0153	0.0192	-0.276	0.255

significantly higher (worse) than the indexes for both the Yung model ($p < 0.001$) and the Calvert model with $f = 0.31$ ($p < 0.01$). Finally, the performance indexes for the Yung model and the Calvert model with $f = 0.31$ were not significantly different ($p > 0.89$).

The poor overall performance of the Calvert model with $f = 0.25$ was in part because it is less sophisticated than the other models and uses more assumptions. Adjusting the correlative parameter f from its recommended value of 0.25 (18) to 0.31 made the Calvert model fit our data better. However, the Calvert model is limited as a predictive model in that it is semiempirical. For a different set of experiments, the optimal f may not be 0.31.

Underestimation of penetration by the Boll model may have been caused by several model deficiencies: (1) For one of the venturi scrubbers used in our experiments, approximately 20% of the liquid was found not to be available for particle collection because it was on the walls rather than dispersed as droplets (26). (2) The Sauter mean droplet diameter predicted by the Nukiyama-Tanasawa equation (16) may be inappropriate for calculation of penetration in a venturi scrubber. For one of the venturi scrubbers used, our experimental measurements indicated that the Nukiyama-Tanasawa equation underestimated the Sauter mean diameter significantly; the predicted droplet diameter from eq 3 was 100 μm , whereas the average measured diameter was about 400 μm (26). A 400- μm droplet would result in a prediction of penetration significantly higher than would a 100- μm droplet (27, 28). (3) The liquid may reach an appreciable velocity prior to atomization, and thus some of its sweeping action occurs while its surface area is minimal. In our experiments, water was injected slightly upstream of the converging-section entrance, but most atomization may have taken place in the throat. Thus, because Boll assumed atomization occurs immediately after injection, much of the particle collection in the converging section predicted from the Boll model may have not taken place. Underestimation of penetration by the Boll model has been observed previously; Boll compared his model with the data of Ekman and Johnstone (6) and Brink and Contant (29) and found that, as in the present work, it often underestimated penetration.

The first two of the above-stated deficiencies also affect the validity of the Yung model. Although the Yung model predicted penetration with less bias than the Boll model, as evidenced by the magnitude of $\bar{\Delta}$ in Table I, this may have been fortuitous; because the Yung model accounts only for particle collection in the throat, this would tend to overestimate penetration and offset the effect of the above-stated deficiencies.

Effect of Throat Diameter. The comparisons of data with models were examined for the influence of throat diameter. For each throat diameter, Table II gives values of $\bar{\Delta}$ and I for each model. All model predictions improve with increasing throat diameter, particularly for the Calvert model. For each model, the performance indexes were lowest (best) for the large throat and highest (worst) for the small throat. Comparisons between throat diameters for all models were statistically significant ($p < 0.05$), except for the comparison between medium and large throats

using the Yung model. In addition, predictions for the small throat tended to overestimate measured penetrations greatly, as shown by the sign and magnitude of $\bar{\Delta}$, whereas predictions for the medium and large throats were, on average, less biased. Calvert et al. (8) conducted experiments using three different venturis and decided to discard data from their smallest venturi (25 mm diameter throat) because of experimental difficulties. In their opinion, it was "very difficult to get good data on such a small venturi."

Conclusions

Of the three models investigated, the model of Yung et al. (9) is probably best for most applications because it is an explicit algebraic expression and gave the best results of the models tested. The model of Calvert et al. (8) is also an explicit algebraic expression and is easy to use, but its predictions are very dependent on the choice of the correlative parameter, f , and thus should be used with caution. The model of Boll (10) did not give good results in our experiments; it is, however, a better starting point for developing improved predictive models because it is more realistic. Finally, all models tended to give better predictions as throat size increased.

Supplementary Material Available

A summary of operating parameters, pressure drops, and measured penetrations with coefficients of variation for all experimental runs (5 pages) will appear following these pages in the microfilm edition of this volume of the journal. Photocopies of the supplementary material from this paper or microfiche (105 \times 148 mm, 24 \times reduction, negatives) may be obtained from Microforms Office, American Chemical Society, 1155 16th St., N.W., Washington, DC 20036, or directly from the authors. Orders must state whether for photocopy or microfiche and give complete title of article, names of authors, journal issue date, and page numbers. Prepayment, check or money order for \$9.00 for photocopy (\$11.00 foreign) or \$6.00 for microfiche (\$7.00 foreign), is required and prices are subject to change.

Acknowledgments

Stephen Ferguson collected most of the experimental data reported here.

Glossary

- a_d droplet acceleration, m/s^2
- c_b number concentration of particles downstream of venturi scrubber when no challenge aerosol particles generated, m^{-3}
- c_d number concentration of particles downstream of venturi scrubber, m^{-3}
- c_u number concentration of particles upstream of venturi scrubber, m^{-3}
- C_D drag coefficient, dimensionless
- C_{Di} drag coefficient at throat inlet, dimensionless
- C_c Cunningham slip-correction factor for particle, dimensionless
- C_v Coefficient of variation of measured fractional penetration, %
- D_d droplet diameter or Sauter mean diameter, m
- D_p particle diameter, m
- f correlative parameter in model of Calvert et al. (8), dimensionless

I	least-squares performance index (see eq 17), dimensionless	(6) Ekman, F. O.; Johnstone, H. F. <i>Ind. Eng. Chem.</i> 1951, 43, 1358-1363.
K	impaction parameter (ratio of particle stopping distance to droplet diameter), dimensionless	(7) Calvert, S. <i>AIChE J.</i> 1970, 16, 392-396.
K_i	impaction parameter evaluated at gas velocity in throat and zero droplet velocity, dimensionless	(8) Calvert, S.; Lundgren, D.; Mehta, D. S. <i>J. Air Pollut. Control Assoc.</i> 1972, 22, 529-532.
L_t	throat length, m	(9) Yung, S.; Calvert, S.; Barbarika, H. F.; Sparks, L. E. <i>Environ. Sci. Technol.</i> 1978, 12, 456-459.
n	number of measured penetrations, dimensionless	(10) Boll, R. H. <i>Ind. Eng. Chem. Fundam.</i> 1973, 12, 40-50.
N	number of transfer units, dimensionless	(11) Behie, S. W.; Beckmans, J. M. <i>Can. J. Chem. Eng.</i> 1973, 51, 430.
N_m	measured number of transfer units, dimensionless	(12) Taheri, M.; Sheih, C. M. <i>AIChE J.</i> 1975, 12, 153-157.
N_p	predicted number of transfer units, dimensionless	(13) Goel, K. C.; Hollands, K. G. T. <i>Atmos. Environ.</i> 1977, 11, 837-845.
Pt	fractional penetration (fraction of particles in specified size range not collected in venturi scrubber), dimensionless	(14) Placek, T. D.; Peters, L. K. <i>AIChE J.</i> 1981, 27, 984-993.
Q_L	liquid volumetric flow rate, m ³ /s	(15) Placek, T. D.; Peters, L. K. <i>AIChE J.</i> 1982, 28, 31-39.
Q_G	gas volumetric flow rate, m ³ /s	(16) Nukiyama, S.; Tanasawa, Y. <i>Trans. Soc. Mech. Eng. (Tokyo)</i> 1939, 5, 68-75.
Re	droplet Reynolds number, dimensionless	(17) Walton, H. W.; Woolcock, A. <i>Int. J. Air Pollut.</i> 1960, 3, 129.
t	time, s	(18) Calvert, S. In "Air Pollution", 3rd ed.; Stern, A. C., Ed.; Academic Press: New York, 1977; Vol. IV, pp 280-281.
V_d	droplet velocity, m/s	(19) Hollands, K. G. T.; Goel, K. C. <i>Ind. Eng. Chem.</i> 1975, 14, 16-22.
V_{di}	liquid velocity parallel to venturi scrubber axis from injectors, m/s	(20) Lapple, C. E.; Shepard, C. B. <i>Ind. Eng. Chem.</i> 1940, 32, 605-617.
V_{de}^*	ratio of droplet velocity at exit of throat to gas velocity in throat, dimensionless	(21) Dorsch, R. G.; Saper, P. G.; Kadow, C. F. National Advisory Committee on Aeronautics Technical Note 3587, Cleveland, OH, Sept 1955.
V_G	superficial gas velocity, m/s	(22) Ranz, W. E. Pennsylvania State University, Department of Engineering Research Bulletin 66, University Park, PA, Dec 1956.
V_{Gt}	superficial gas velocity in throat, m/s	(23) Fleischer, P. E. In "System Analysis by Digital Computer"; Kuo, F. F., Kaiser, J. F., Eds.; Wiley: New York, 1955; pp 180-203.
x	position along venturi scrubber axis, m	(24) Wilde, D. J.; Beightler, C. S. "Foundations of Optimization"; Prentice-Hall: New York, 1967; pp 288-298.
x_i	position of liquid injectors along venturi scrubber axis, m	(25) Naden, R. A.; Leeds, J. V. <i>Environ. Sci. Technol.</i> 1971, 5, 522-531.
Δ	$N_m - N_p$, dimensionless	(26) Leith, D.; Martin, K. P.; Cooper, D. W. <i>Filt. Sep.</i> , in press.
$\bar{\Delta}$	mean value of $N_m - N_p$	(27) Leith, D.; Cooper, D. W. <i>Atmos. Environ.</i> 1980, 14, 657-663.
η	single-droplet collection efficiency (ratio of number of particles collected by droplet to number of particles whose centers would intersect droplet if streamlines remained straight), dimensionless	(28) Cooper, D. W.; Leith, D. <i>Aerosol Sci. Technol.</i> 1984, 3, 63-70.
ρ_L	liquid density, kg/m ³	(29) Brink, J. A.; Contant, C. E. <i>Ind. Eng. Chem.</i> 1958, 50, 1157-1160.
ρ_G	gas density, kg/m ³	
ρ_p	particle density, kg/m ³	
σ_Δ	standard deviation of Δ	
μ_G	gas viscosity, Pa s	

Literature Cited

- (1) Burchsted, C. A.; Kahn, J. E.; Fuller, A. B. "Nuclear Air Cleaning Handbook"; ERDA 76-21, National Technical Information Service: Springfield, VA, 1976.
- (2) Drew, R. T.; Lippman, M. In "Air Sampling Instruments", 5th ed.; ACGIH Air Sampling Instruments Committee, Ed.; American Conference of Governmental Industrial Hygienists: Cincinnati, OH, 1978; p 130.
- (3) Pinnick, R. G.; Auvermann, H. J. *J. Aerosol Sci.* 1979, 10, 55-74.
- (4) Leith, D.; Martin, K. P. *Am. Ind. Hyg. Assoc. J.* 1984, 45, 242-244.
- (5) Dropp, L. T.; Akbrut, A. J. *Teploenergetika* 1972, 7, 63-68.

Received for review October 11, 1983. Revised manuscript received July 5, 1985. Accepted October 16, 1985. Although the information described in this article has been funded in part by the United States Environmental Protection Agency under grant R809003010 to Harvard University, it has not been subjected to the Agency's required peer and administrative review. Therefore, this paper does not necessarily reflect the views of the Agency and no official endorsement should be inferred.